Electromechanical analysis of a piezoresistive pressure microsensor for low-pressure biomedical applications

A.L. Herrera-May[a,d], B.S. Soto-Cruz[b], F. López-Huerta[c], and L.A. Aguilera Cortés[d]
[a]*Centro de Investigación en Micro y Nanotecnología, Universidad Veracruzana, Boca del Río, Ver., México.*
[b]*Centro de Investigación en Dispositivos Semiconductores, Benemérita Universidad Autónoma de Puebla, Puebla, Pue., México.*
[c]*Facultad de Ciencias Físico Matemáticas, Benemérita Universidad Autónoma de Puebla, Puebla, Pue., México.*
[d]*Departamento Ingeniería Mecánica, Campus Irapuato-Salamanca, Universidad de Guanajuato, Salamanca, Gto. México.*

Recibido el 9 de junio de 2008; aceptado el 12 de enero de 2009

The electromechanical analysis of a piezoresistive pressure microsensor with a square-shaped diaphragm for low-pressure biomedical applications is presented. This analysis is developed through a novel polynomial model and a finite element method (FEM) model. A microsensor with a diaphragm 1000 μm length and with three different thicknesses (10, 15, and 20 μm) is studied. The electric response of this microsensor is obtained with a Wheatstone bridge of four p-type piezoresistors located on the diaphragm surface. The diaphragm that is 10 μm thick exhibits a maximum deflection of 3.74 μm using the polynomial model, which has a relative difference of 5.14 and 0.92% with respect to the Timoshenko model and the FEM model, respectively. The maximum sensitivity and normal stress calculated using the polynomial model are 1.64 mV/V/kPa and 102.1 MPa, respectively. The results of the polynomial model agree well with the Timoshenko model and FEM model for small deflections. In addition, the polynomial model can be easily used to predict the deflection, normal stress, electric response and sensitivity of a piezoresistive pressure microsensor with a square-shaped diaphragm under small deflections.

Keywords: Finite element model; piezoresistors; polynomial model; pressure microsensor.

El análisis electromecánico de un microsensor de presión piezoresistivo con un diafragma de sección cuadrada para aplicaciones biomédicas de baja presión es presentado. Este análisis es desarrollado mediante un nuevo modelo polinomial y un modelo con el método elemento finito (FEM). Un microsensor con un diafragma de 1000 μm de longitud y tres diferentes espesores (10, 15 y 20 μm) es estudiado. La respuesta eléctrica de éste microsensor es obtenida mediante un puente de Wheatstone con cuatro piezoresistores tipo p localizados sobre la superficie del diafragma. El diafragma con 10 μm de espesor presenta una deflexión máxima de 3.74 μm utilizando el modelo polinomial, el cual tiene una diferencia relativa de 5.14 and 0.92% con respecto al modelo de Timoshenko y al modelo FEM, respectivamente. La máxima sensibilidad y esfuerzo normal calculado con el modelo polinomial son 1.64 mV/V/kPa and 102.1 MPa, respectivamente. Los resultados del modelo polinomial concuerdan bien con el modelo de Timoshenko y el modelo FEM para pequeñas deflexiones. Además, el modelo polinomial puede ser utilizado fácilmente para predecir la deflexión, esfuerzo normal, respuesta eléctrica y sensibilidad de un microsensor de presión piezoresistivo con un diafragma de sección cuadrada sujeto a pequeñas deflexiones.

Descriptores: Modelo de elemento finito; piezoresistores; modelo polinomial; microsensor de presión.

PACS: 07.10.Cm; 07.07.Df; 47.11.Fg

1. Introduction

Pressure microsensors are widely used in automotive applications, process control and biomedical applications [1]. Pressure microsensors used in biomedical applications include the measurement of blood pressure [2], intraocular eye pressure [3], intracranial pressure, pulse rate, intrauterine pressure, abdominal and urinary pressure [4-5]. For many biomedical applications, the capacitive detection technique is used mainly due to its high sensitivity. However, the capacitive pressure microsensors have problems with the hermetic vacuum sealing of the capacitive cavity, the electrical lead transfer between the vacuum-sealed cavity and the outside world [6], the high cost due to the complex fabrication process and the difficult to use post-end circuits to compensate the low linearity of these microsensors [7]. To overcome these problems, piezoresistive pressure microsensors are an other option for designers and researchers because these microsensors are easy to use and to fabricate [8-9]. In addition, the low sensitivity of piezoresistive pressure microsensors can be improved by integrating amplifier circuits [10].

The pressure microsensors often use a thin square-shaped diaphragm as their main sensor element. This is because of its compatibility with bulk and surface silicon micromachining processes [11-12]. A pressure applied on the diaphragm generates an increase in its deflection until the elastic force is balanced by the pressure. The pressure range that can be measured by the diaphragm depends on its dimensions (surface area and thickness), geometry, edge conditions, and material [13]. For example, in biomedical applications to measure the blood pressure and heart rate, pressure microsensors are required to operate in the range of 0-40 kPa (0-300 mmHg) [14].

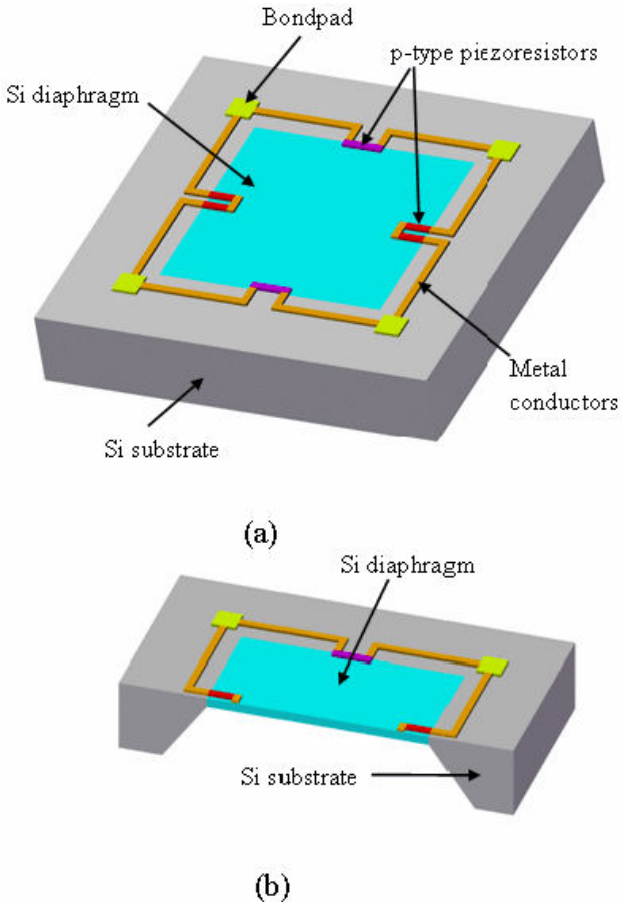

FIGURE 1. (a) Complete and b) cross-sectional views of a piezoresistive microsensor with a square-shaped diaphragm.

The diffused resistors on the silicon substrate are used to measure the strain of the diaphragm of the pressure microsensors. This piezoresistive microsensor generally has four piezoresistors in a Wheatstone bridge configuration to measure the stresses in a silicon diaphragm under normal pressure [15].

The electromechanical behavior of piezoresistive pressure microsensors is predicted during the design phase. This design is used to find the maximum electromechanical performance of the microsensors to improve their sensitivity and resolution. In the past, the electromechanical design of these devices has often been studied with the Timoshenko model for plates [16-17] and finite element method (FEM) models [18-19]. However, the Timoshenko model contains complicated terms and FEM models need considerable computing time. Furthermore, the accuracy of a FEM model depends on the shape and size of mesh used in these models; thus, FEM models are difficult to use between designers and researches. Therefore, simple theoretical models are needed to decrease the design time of pressure microsensors for biomedical applications. In order to solve this problem, this paper presents a novel polynomial model for an easier and faster prediction of the electromechanical behavior of a piezoresistive pressure microsensor with a thin square-shaped diaphragm, which is proposed to measure the blood pressure and heart rate.

The paper is organized as follows. In Sec. 2, a novel polynomial model for predicting the electromechanical behavior of a piezoresistive pressure microsensor with a square-shaped diaphragm is developed. This model is obtained with the small-deflection theory for the bending of plates and the Ritz method. In addition, the electromechanical response calculated with the polynomial model is compared with the Timoshenko model for plates. In Sec. 3, the discussion of the electromechanical behavior of a piezoresistive pressure microsensor obtained with the polynomial model, Timoshenko model, and FEM model is presented.

2. Pressure microsensor design

The mechanical and electric design of a piezoresistive pressure microsensor with a square-shaped diaphragm to measure blood pressure and heart rate is need to improve its electromechanical performance. Therefore, this design will help in choosing the dimensions of the microsensor with the best sensitivity and resolution for these biomedical applications.

2.1. Mechanical design

The diaphragm of a piezoresistive pressure microsensor can be modeled as a square plate with four edges clamped under a uniform normal pressure. In this work, the thin diaphragm of the piezoresistive pressure microsensor is considered as a thin plate with edges clamped. A plate is called "thin" when its ratio of thickness to the smaller span length is less than 1/20 [20]. Figure 1 shows the complete and cross-sectional views of a typical piezoresistive pressure microsensor with a thin square-shaped diaphragm. This microsensor has a Wheatstone bridge with four p-type piezoresistors, which are located near the edges of the diaphragm. The diaphragm and piezoresistors are aligned with the (110) directions in the $\langle 100 \rangle$ crystallographic plane.

The governing equation of the deflection and normal stress of a thin diaphragm is derived considering the fundamental assumptions (also known as Kirchhoff assumptions) of the small-deflection theory for the bending of thin plates, which are stated as follows [20]:

1. The material of the plate is elastic, homogeneous, and isotropic.

2. The plate is initially flat.

3. The deflection of the midsurface is small compared with the thickness of the plate and a maximum deflection of one-fifth of its thickness is considered the limit of the small-deflection theory. The slope of the deflected surface is very small and the square of the slope is a negligible quantity with respect to unity.

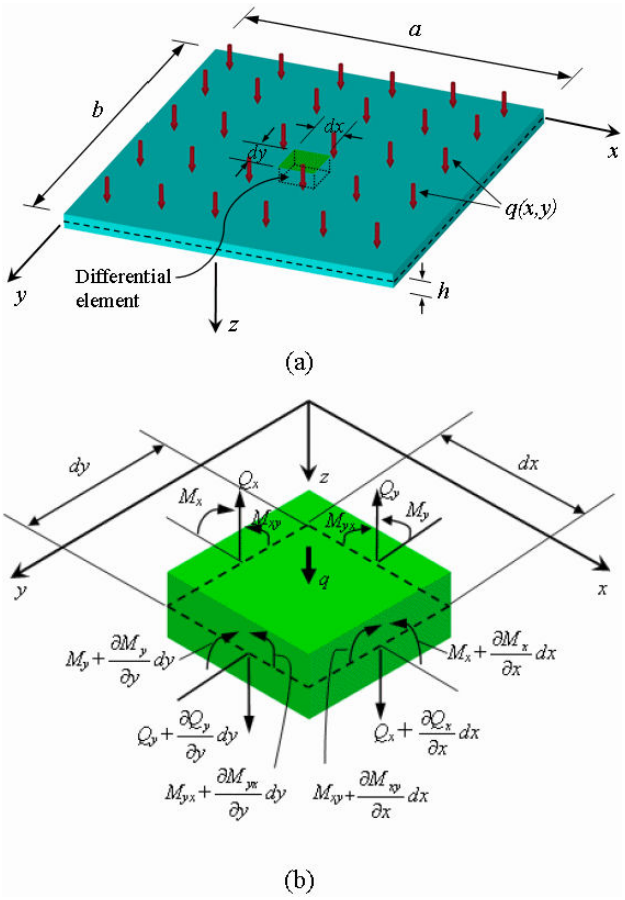

FIGURE 2. a) Schematic diagram of a rectangular-shaped diaphragm under an uniform normal pressure and, b) forces and moments on a differential element of the diaphragm.

4. The straight lines, normal to the midsurface before bending, remain straight and normal to the midsurface during the strain, and the length of such elements is not altered. This means that the vertical shear strains γ_{xz} and γ_{yz} can be neglected.

5. Since the deflection of a plate is small, it is assumed that the midsurface remains unstrained after bending.

6. The normal stress to the midsurface (σ_z) is small compared with the other stress components and can be neglected.

The diaphragm is strained when an uniform normal pressure, $q(x,y)$, is applied on the diaphragm surface, as shown in Fig. 2a. This strain causes normal (σ_x, σ_y, σ_{xz}, and σ_{yz}) and shear stresses (τ_{xz} and τ_{yz}) on the diaphragm. In addition, the bending (M_x, M_y) and twisting moments (M_{xy}) per unit length of the diaphragm midsurface, as well as the shear forces (Q_x, Q_y) per unit of length of the diaphragm midsurface, can be expressed in terms of the normal (σ_x and σ_y) and shear stresses (τ_{xy}, τ_{xz} and τ_{yz}) [21]. That is,

$$\left\{ \begin{array}{c} M_x \\ M_y \\ M_{xy} \end{array} \right\} = \int_{-\frac{h}{2}}^{\frac{h}{2}} \left\{ \begin{array}{c} \sigma_x \\ \sigma_y \\ \tau_x y \end{array} \right\} z dz,$$

$$\left\{ \begin{array}{c} Q_x \\ Q_y \end{array} \right\} = \int_{-\frac{h}{2}}^{\frac{h}{2}} \left\{ \begin{array}{c} \tau_{xz} \\ \tau_{yz} \end{array} \right\} dz, \qquad (1)$$

where z is the vertical distance measured from the diaphragm midsurface.

Based on the reciprocity law of shear stresses (τ_{xy} and τ_{yx}), the twisting moments on perpendicular faces of a diaphragm element are identical, *i.e.*, M_{xy}=M_{yx}. It is important to mention that while the theory of thin plates omits the effect of the strain components γ_{xz} and γ_{yz} on bending, the vertical shear forces Q_x and Q_y are not negligible.

Figure 2b shows the equilibrium of an element cut out of a diaphragm, under a distributed load, by two pairs of planes parallel to the *xz* and *yz* planes, since the stress-resultants and stress-couples are considered at the midsurface of this element. Note that as this element is very small, the force and moment components are distributed uniformly on the midsurface of the diaphragm element. Projecting all the forces on the element in the z-axis, the following equations of equilibrium are obtained [21]:

$$\begin{aligned} \frac{\partial Q_x}{\partial x} + \frac{\partial Q_y}{\partial y} + q &= 0 \\ \frac{\partial M_{xy}}{\partial x} + \frac{\partial M_y}{\partial y} - Q_y &= 0 \\ \frac{\partial M_{xy}}{\partial y} + \frac{\partial M_x}{\partial x} - Q_x &= 0, \end{aligned} \qquad (2)$$

where $q(x$,y) is a uniform load applied at the diaphragm surface. From equation set (2), the relation between the uniform load and the bending moment can be rewritten as [21]

$$\frac{\partial^2 M_x}{\partial x^2} + 2\frac{\partial^2 M_{xy}}{\partial x \partial y} + \frac{\partial^2 M_y}{\partial y^2} = -q. \qquad (3)$$

Substituting equation set (1) into (3), a relation between normal stress and uniform load can be obtained as

$$\int_{-\frac{h}{2}}^{\frac{h}{2}} \left(\frac{\partial^2 \sigma_x}{\partial x^2} + 2\frac{\partial^2 \sigma_{xy}}{\partial x \partial y} + \frac{\partial^2 \sigma_y}{\partial y^2} \right) z dz = -q. \qquad (4)$$

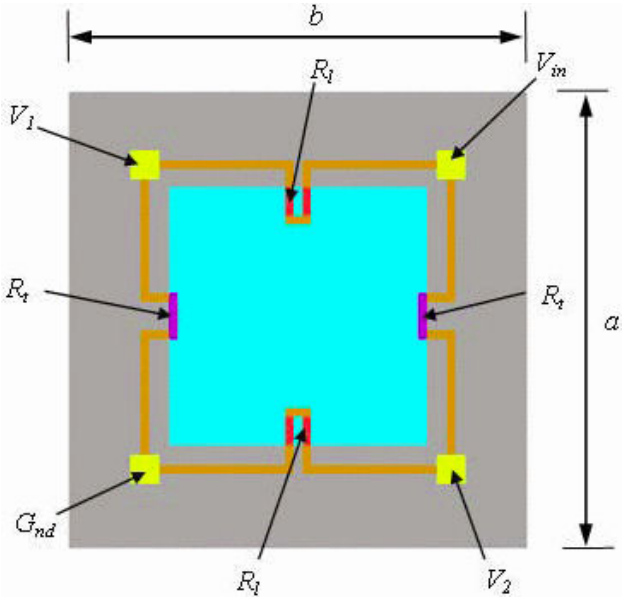

FIGURE 3. Top view of a Wheatstone bridge with four p-type piezoresistors on the diaphragm surface of a pressure microsensor.

Considering the Kirchhoff assumptions for the bending of thin plates (diaphragms) expressed above, the stress in the z-direction and stress components (σ_x, σ_y, and σ_{xy}) can be written in a matrix form given by

$$\begin{bmatrix} \sigma_x \\ \sigma_y \\ \sigma_{xy} \end{bmatrix} = \frac{Ez}{1-\nu^2} \begin{bmatrix} 1 & \nu & 0 \\ \nu & 1 & 0 \\ 0 & 0 & 1-\nu \end{bmatrix} \begin{bmatrix} \frac{\partial^2 w}{\partial x^2} \\ \frac{\partial^2 w}{\partial y^2} \\ \frac{\partial^2 w}{\partial x \partial y} \end{bmatrix}, \quad (5)$$

where E is Young's modulus, ν is Poisson's ratio of the diaphragm material, and w is vertical deflection of the diaphragm.

The deflection $w(x,y)$ with respect to the load intensity $q(x,y)$ can be obtained by substituting Eq. (5) into Eq. (4);

$$\left(\frac{\partial^4}{\partial x^4} + 2\frac{\partial^4}{\partial x^2 \partial y^2} + \frac{\partial^4}{\partial y^4}\right) w = \frac{q}{D}, \quad (6)$$

where D is the flexural stiffness per unit length of the thin diaphragm.

A thin diaphragm exhibits greater stiffness than a beam by a factor 1/(1-v^2). This flexural stiffness per unit length is given by

$$D = \int_{-\frac{h}{2}}^{\frac{h}{2}} \frac{Ez^2}{1-v^2} dz = \frac{Eh^3}{12(1-v^2)}. \quad (7)$$

The analytical equations to solve the Eq. (6) must satisfy the following boundary conditions of a clamped diaphragm:

$$\begin{aligned} w = 0 \quad \frac{\partial w}{\partial x} = 0 \quad (x = 0, x = a) \\ w = 0 \quad \frac{\partial w}{\partial y} = 0 \quad (y = 0, y = b). \end{aligned} \quad (8)$$

The solution of the partial differential Eq. (6) is complicated and this solution is needed to find the deflection and the normal stress components of the diaphragm. Double trigonometric-series solutions can be used to solve Eq. (6), but they generally are not easy to use [22]. However, the polynomial solutions are the simplest equations to solve equations similar to Eq. (6); however, they must be obtained carefully to satisfy the boundary conditions indicated by Eq. (8) and to keep acceptable accuracy. Therefore, in this work a novel polynomial model is proposed for solving Eq. (6) with the boundary conditions of a clamped diaphragm. Thus, the proposed polynomial model is given by

$$w(x,y) = \sum_{m=1}^{r}\sum_{n=1}^{s} c_{mn} \left[1 - \frac{x}{a}\right]^2 \times \left[1 - \frac{y}{b}\right]^2 \left(\frac{x}{a}\right)^{2m} \left(\frac{y}{b}\right)^{2n}, \quad (9)$$

where w is the deflection, c_{mn} represents coefficients to be determined, a and b are the lengths of the diaphragm edges.

The novel polynomial model satisfies the boundary conditions indicated by Eq. (8) and contains two series of polynomial terms. These polynomial terms have unknown coefficients c_{mn} that can be found by variational methods. The polynomial model considers the deflection of a diaphragm as the superposition of polynomial curves of order $2m$ and $2n$ in the x- and y- directions. Furthermore, the r and s terms indicate the maximum number of polynomial curves in the x- and y- directions to use in the polynomial model. The maximum value of these terms (r and s) will depend on the designer and the variational method used to find the coefficients c_{mn}.

The Ritz method is a variational method based on the principle of minimum potential energy to solve boundary value problems of plates. In this work, the Ritz method is considered to find the coefficients c_{mn} of the polynomial model. First, this model is applied to a pressure microsensor with a rectangular-shaped diaphragm and afterwards is simplified to a square-shaped diaphragm. Therefore, the Ritz method is applied to a rectangular-shaped diaphragm with sides a and b under a uniform surface load. Thus, the strain energy U associated with the bending of the diaphragm is given by [22]

$$U = \frac{1}{2}\int\int_A D\left\{\left(\frac{\partial^2 w}{\partial x^2} + \frac{\partial^2 w}{\partial y^2}\right)^2 - 2(1-v) \times \left[\frac{\partial^2 w}{\partial x^2}\frac{\partial^2 w}{\partial y^2} - \left(\frac{\partial^2 w}{\partial x \partial y}\right)^2\right]\right\} dxdy, \quad (10)$$

where A is the area of the diaphragm surface.

The work done by the surface load $q(x,y)$ is

$$W = \int\int_A wq dxdy \quad . \quad (11)$$

The potential energy equation is obtained by $\Pi = U - W$:

$$\Pi = \int\int_A \left\{ \frac{D}{2} \left[\left(\frac{\partial^2 w}{\partial x^2} + \frac{\partial^2 w}{\partial y^2} \right)^2 - 2(1-v) \times \left[\frac{\partial^2 w}{\partial x^2}\frac{\partial^2 w}{\partial y^2} - \left(\frac{\partial^2 w}{\partial x \partial y} \right)^2 \right] \right] - wq \right\} dxdy \quad . \quad (12)$$

Assuming the boundary conditions given by Eq. (8) and integrating the last term of Eq. (10) by parts, then the strain energy U is reduced to

$$U = \frac{D}{2} \int\int_A \left(\frac{\partial^2 w}{\partial x^2} + \frac{\partial^2 w}{\partial y^2} \right)^2 dxdy. \quad (13)$$

Introducing Eq. (9) into Eq. (13) yields

$$U = \int_0^b \int_0^a \left\{ \sum_{m=1}^{r} \sum_{n=1}^{s} c_{mn} \left(\frac{x}{a}\right)^{2m} \left(\frac{y}{b}\right)^{2n} \times \left[\left[1-\frac{y}{b}\right]^2 \left(\frac{2m(2m-1)}{a^2} \left[1-\frac{x}{a}\right]^2 \left(\frac{x}{a}\right)^{-2} - \frac{8m}{a^2}\left[1-\frac{x}{a}\right]\left(\frac{x}{a}\right)^{-1} + \frac{2}{a^2} \right) + \left[1-\frac{x}{a}\right]^2 \left(\frac{2n(2n-1)}{b^2} \left[1-\frac{y}{b}\right]^2 \left(\frac{y}{b}\right)^{-2} - \frac{8n}{b^2}\left[1-\frac{y}{b}\right]\left(\frac{y}{b}\right)^{-1} + \frac{2}{b^2} \right) \right] \right\}^2 dxdy \quad (14)$$

The work done by the uniform surface load $q(x,y) = q_0$ on a rectangular-shaped diaphragm is calculated by

$$W = q_0 \int_0^b \int_0^a \sum_{m=1}^{r} \sum_{n=1}^{s} c_{mn} \left[1-\frac{x}{a}\right]^2 \times \left[1-\frac{y}{b}\right]^2 \left(\frac{x}{a}\right)^{2m} \left(\frac{y}{b}\right)^{2n} dxdy. \quad (15)$$

Then, Eqs. (14) and (15) are substituted into Eq. (12) and the unknown coefficients c_{mn} are determined by the minimum potential energy principle. Thus,

$$\frac{\partial \Pi}{\partial c_{mn}} = 0. \quad (16)$$

We use the first value of r and s of the polynomial model to obtain the simplest expression of c_{mn}; consequently, the coefficient c_{11} is obtained as

$$c_{11} = \frac{49a^4b^4q_0}{8D(7b^4+4a^2b^2+7a^4)}. \quad (17)$$

Then, the deflection obtained with the polynomial model is given by

$$w = \frac{49a^4b^4q_0}{8D(7b^4+4a^2b^2+7a^4)} \times \left[1-\frac{x}{a}\right]^2 \left[1-\frac{y}{b}\right]^2 \left(\frac{x}{a}\right)^2 \left(\frac{y}{b}\right)^2. \quad (18)$$

For the case of a square-shaped diaphragm ($a = b$), the maximum deflection (w_{max}) is found at its center:

$$w_{\max} = \frac{49q_0a^4}{36864D}. \quad (19)$$

The normal stress components (σ_x and σ_y) of a rectangular-shaped diaphragm are found through the substitution of Eq. (18) into Eq. (5):

$$\sigma_x = \frac{147a^2b^2zq_0}{h^3(7b^4+4a^2b^2+7a^4)} \left\{ b^2\left(1-\frac{y}{b}\right)^2\left(\frac{y}{b}\right)^2 \left[\left(\frac{x}{a}\right)^2 - \frac{4x}{a}\left(1-\frac{x}{a}\right) + \left(1-\frac{x}{a}\right)^2 \right] + a^2 v \left(1-\frac{x}{a}\right)^2\left(\frac{x}{a}\right)^2 \times \left[\left(\frac{y}{b}\right)^2 - \frac{4y}{b}\left(1-\frac{y}{b}\right) + \left(1-\frac{y}{b}\right)^2 \right] \right\}. \quad (20)$$

$$\sigma_y = \frac{147a^2b^2zq_0}{h^3(7b^4+4a^2b^2+7a^4)} \left\{ b^2 v\left(1-\frac{y}{b}\right)^2\left(\frac{y}{b}\right)^2 \left[\left(\frac{x}{a}\right)^2 - \frac{4x}{a}\left(1-\frac{x}{a}\right) + \left(1-\frac{x}{a}\right)^2 \right] + a^2 \left(1-\frac{x}{a}\right)^2\left(\frac{x}{a}\right)^2 \times \left[\left(\frac{y}{b}\right)^2 - \frac{4y}{b}\left(1-\frac{y}{b}\right) + \left(1-\frac{y}{b}\right)^2 \right] \right\}. \quad (21)$$

The maximum normal stresses are found at the middle edges of the rectangular-shaped diaphragm at its upper surface ($z = h/2$) and are given by

$$\sigma_{x\max} = \frac{147a^2b^4q_0}{32h^2(7b^4+4a^2b^2+7a^4)}$$
$$\sigma_{y\max} = \frac{147a^4b^2q_0}{32h^2(7b^4+4a^2b^2+7a^4)}. \quad (22)$$

The maximum normal stresses for a square-shaped diaphragm are found with the substitution $a = b$ into Eq. (22).

The Timoshenko model [23] for a rectangular-shaped plate under small deflections is used to compare its results in relation to the polynomial model. Based on the small-deflection theory for the bending of plates, Timoshenko [23] assumed the total deflection of a rectangular-shaped plate with clamped edges as the sum of three components:w_1, w_2, and w_3. The first component, w_1, comes from the deflection of a simply supported plate under the same pressure load. The following equations are derived for a rectangular-shaped plate (a and b width) under a pressure q_0. In addition, the coordinate system used in these equations is located in the

center of the rectangular-shaped plate. Therefore,

$$w_1=\frac{4q_0a^4}{\pi^5 D}\sum_{m=1,3,5,\ldots}^{\infty}\frac{(-1)^{(m-1)/2}}{m^5}\cos\left(\frac{m\pi x}{a}\right)\times\left[1-\frac{\alpha_m\tanh\alpha_m+2}{2\cosh\alpha_m}\cosh\left(\frac{m\pi y}{a}\right)+\frac{1}{2\cosh\alpha_m}\left(\frac{m\pi y}{a}\right)\sinh\left(\frac{m\pi y}{a}\right)\right] \quad (23)$$

$$w_2=\frac{-a^2}{2\pi^2 D}\sum_{m=1,3,5,\ldots}^{\infty}\frac{E_m(-1)^{(m-1)/2}}{m^2\cosh\alpha_m}\times\cos\left(\frac{m\pi x}{a}\right)\left[\frac{m\pi y}{a}\sinh\left(\frac{m\pi y}{a}\right)-\alpha_m\tanh\alpha_m\cosh\left(\frac{m\pi y}{a}\right)\right] \quad (24)$$

$$w_3=\frac{-b^2}{2\pi^2 D}\sum_{m=1,3,5,\ldots}^{\infty}\frac{E_m(-1)^{(m-1)/2}}{m^2\cosh\beta_m}\times\cos\left(\frac{m\pi y}{b}\right)\left[\frac{m\pi x}{b}\sinh\left(\frac{m\pi x}{b}\right)-\beta_m\tanh\beta_m\cosh\left(\frac{m\pi x}{b}\right)\right], \quad (25)$$

whereE_m and F_m are coefficients to be determined. Also,

$$\alpha_m=\frac{m\pi b}{2a}\qquad\text{and}\qquad\beta_m=\frac{m\pi a}{2b}. \quad (26)$$

Hence, the total deflection of a rectangular-shaped diaphragm (plate) under small deflections is calculated by

$$w_t=w_1+w_2+w_3. \quad (27)$$

The values of E_m and F_m can be obtained by the following equations:

$$\frac{4q_0a^2\alpha_n}{\pi^3n^4\cosh^2\alpha_n}-\tanh\alpha_n=\frac{E_n}{n}\left(\tanh\alpha_n+\frac{\alpha_n}{\cosh^2\alpha_n}\right)+\frac{8na}{\pi b}\sum_{m=1,3,5,\ldots}^{\infty}F_m\frac{1}{m^3\left(\frac{a^2}{b^2}+\frac{n^2}{m^2}\right)} \quad (28)$$

$$\frac{4q_0b^2\beta_n}{\pi^3n^4\cosh^2\beta_n}-\tanh\beta_n=\frac{F_n}{n}\left(\tanh\beta_n+\frac{\beta_n}{\cosh^2\beta_n}\right)+\frac{8nb}{\pi a}\sum_{m=1,3,5,\ldots}^{\infty}E_m\frac{1}{m^3\left(\frac{a^2}{b^2}+\frac{n^2}{m^2}\right)}. \quad (29)$$

For the case of a square-shaped diaphragm, the following assumptions are considered: $E_n=F_n$ and the Eqs. (28) and (29) are same. Therefore, Eqs. (28) and (29) are reduced to

$$\frac{E_n}{n}\left(\tanh\alpha_n+\frac{\alpha_n}{\cosh^2\alpha_n}\right)+\frac{8n}{\pi}\sum_{m=1,3,5,\ldots}^{\infty}\frac{E_m}{m^3}\times\frac{1}{\left(1+\frac{n^2}{m^2}\right)^2}=\frac{4q_0a^2}{\pi^3n^3}\left(\frac{\alpha_n}{\cosh^2\alpha_n}-\tanh\alpha_n\right). \quad (30)$$

The coefficients E_m can be determined by the method of successive approximations. Only the first four coefficients (E_1, E_3, E_5, and E_7) were considered because a greater increase in these terms does not significantly increase the accuracy of the Timoshenko model [23]; thus, E_1=0.3722K, E_3=−0.0380K, E_5=−0.0178K and E_7=−0.0085K, where

$$K=-\frac{4q_0a^2}{\pi^3}. \quad (31)$$

The normal stress components of a square-shaped plate can be determined by Eq. (5), considering these four coefficients (E_1, E_3, E_5 and E_7).

In the next section, the electric design of the piezoresistive pressure microsensor is presented.

2.2. Electric design

The piezoresistive pressure microsensor has a Wheatstone bridge with four p-type piezoresistors on the diaphragm surface, as shown in Fig. 3. Two pairs of piezoresistors are placed on opposite sides of the edges of the diaphragm to increase its sensitivity to an applied pressure. Accordingly, two piezoresistors are in parallel with the maximum normal stress (σ_x) and the other two are perpendicular to σ_x. For a piezoresistor subjected to parallel and perpendicular stress components (σ_l and σ_t), the change in resistance is [24]

$$\frac{\Delta R}{R}=\pi_l\sigma_l+\pi_t\sigma_t, \quad (32)$$

where π_l and π_t are the piezoresistive coefficients parallel and perpendicular to the piezoresistor length.

The values of the piezoresistive coefficients depend on the orientation of the wafer and the diaphragm, the type and concentration of doping, and temperature [25]. For the (110) directions in the $\langle 100\rangle$ crystallographic plane, the parallel and perpendicular piezoresistive coefficients are given by [24]

$$\pi_l=\pi_{11}-2\left(\pi_{11}-\pi_{12}-\pi_{44}\right)\left(\frac{1}{4}\right)$$

$$\pi_t=\pi_{12}+\left(\pi_{11}-\pi_{12}-\pi_{44}\right)\left(\frac{1}{2}\right) \quad (33)$$

where π_{11}, π_{12} and π_{44} are the fundamental cubic piezoresistive coefficients. This work considered a resistivity of 7.8 Ω cm for the wafer, p-type piezoresistors with π_{11}=6.6×10^{-11}Pa^{-1}, π_{12}=−1.1×10^{-11}Pa^{-1} and π_{44}=138.1 × 10^{-11}Pa^{-1}[15]. Thus, the parallel and perpendicular piezoresistive coefficients are π_l=71.8 × 10^{-11}Pa^{-1} and π_t= − 66.3 × 10^{-11}Pa^{-1}. Besides, E= 169.8 GPa was considered for the silicon and Poisson's ratio ν=0.066 [24].

The output voltage, ΔV, of the Wheatstone bridge with a supply voltage, V_{in}, is given by [24]

$$\frac{\Delta V}{V_{in}}=\frac{(\Delta R/R)_l-(\Delta R/R)_t}{2+(\Delta R/R)_l+(\Delta R/R)_t} \quad (34)$$

where

$$\left(\frac{\Delta R}{R}\right)_l=\pi_l\sigma_l+\pi_t\sigma_t\qquad\left(\frac{\Delta R}{R}\right)_t=\pi_l\sigma_t+\pi_t\sigma_l. \quad (35)$$

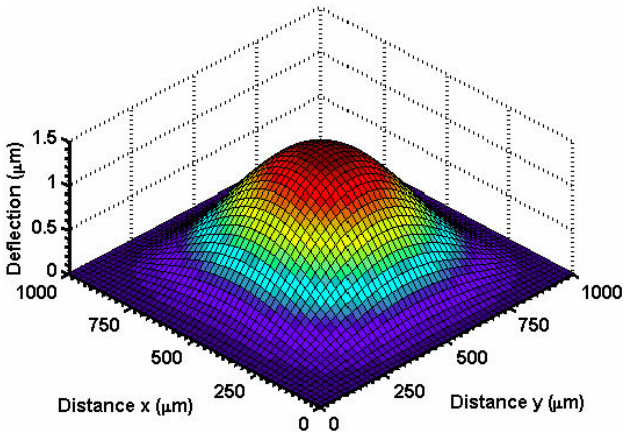

FIGURE 4. Absolute deflection of a square-shaped diaphragm (1000 μm length and 10 μm thickness) obtained with the novel polynomial model for an uniform normal pressure of 15 kPa.

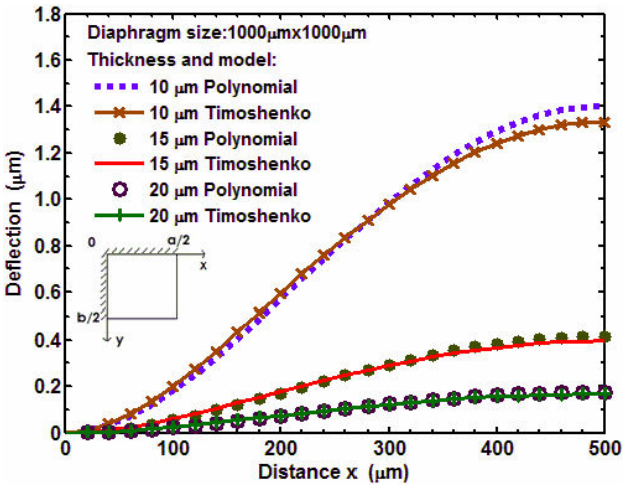

FIGURE 5. Deflection distribution at the middle (y=b/2) of one quadrant of a square-shaped diaphragm (1000 μm length) considering three different thicknesses (10 μm, 15 μm, and 20 μm) and an uniform normal pressure of 15 kPa.

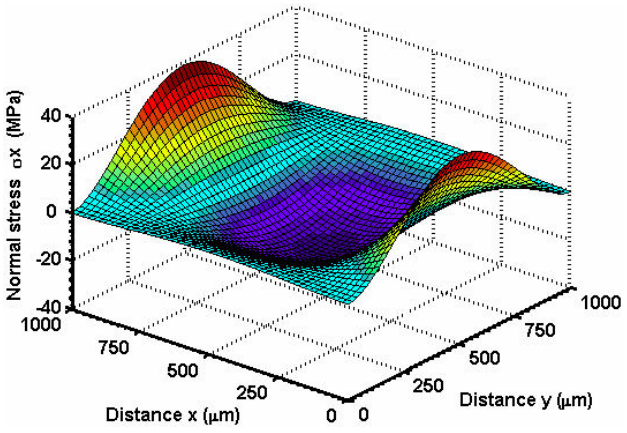

FIGURE 6. Normal stress distribution of a piezoresistive pressure microsensor with a square-shape diaphragm (1000 μm length and 10 μm thickness) under an uniform normal pressure of 15 kPa.

The parallel and perpendicular stress components are calculated using

$$\sigma_l = \sigma_x(0, b/2) \quad \sigma_t = \sigma_x(a/2, 0). \tag{36}$$

The sensitivity, S, of the pressure microsensor can be determined by the following equation:

$$S = \frac{\Delta V/V_{in}}{q_0}, \tag{37}$$

where q_0 is the uniform-normal pressure on the diaphragm surface.

3. Results and discussion

This section shows the result of the relations between the size, pressure, deflection, normal stress components and electric response of a piezoresistive pressure microsensor proposed to measure blood pressure and heart rate. This microsensor has a square-shaped silicon diaphragm 1000 μm length and in three different thicknesses (10, 15, and 20 μm) under a uniform normal pressure. The pressure range considered for the electromechanical analysis of this microsensor was 0-40 kPa (0-300 mmHg) [14]. The electromechanical response was obtained with the novel polynomial model, which agrees well with the Timoshenko model and FEM model for small deflections. In addition, this polynomial model predicts the electromechanical behavior of the piezoresistive pressure microsensor more easily and quickly.

Figure 4 shows the absolute amplitude of the deflection distribution of a square-shaped diaphragm (1000 μm length and 10 μm thickness) of the pressure microsensor, which is obtained with the proposed polynomial model. This deflection distribution is caused by a uniform normal pressure (15 kPa) on the diaphragm's external surface. The maximum deflection (1.40 μm) is located at the center of this diaphragm. In addition, the absolute deflection distribution over the middle (y=b/2) of one quadrant (due to symmetry) of this diaphragm is found using the polynomial model and Timoshenko model, as shown in Fig. 5. For this case three thicknesses (10, 15, and 20 μm) are considered, and a uniform normal pressure of 15 kPa on the diaphragm. The maximum deflection (1.40 μm) is less than one-fifth (2 μm) of the smallest thickness (10 μm), which satisfies the condition for small deflections [23]. The deflections obtained by the model polynomial agree well with the results of the Timoshenko model.

Figure 6 indicates the normal stress distribution (σ_x) of the same square-shaped diaphragm 10 μm thick as a function of x and y distances, respectively. This stress distribution was calculated using the polynomial model Eq. (20) and considering a pressure of 15 kPa on the diaphragm. The maximum stresses (38.28 MPa) are found at the middle edges ($x = 0$, $y = 500$ μm and $x = 1000$ μm, $y = 500$ μm) of the

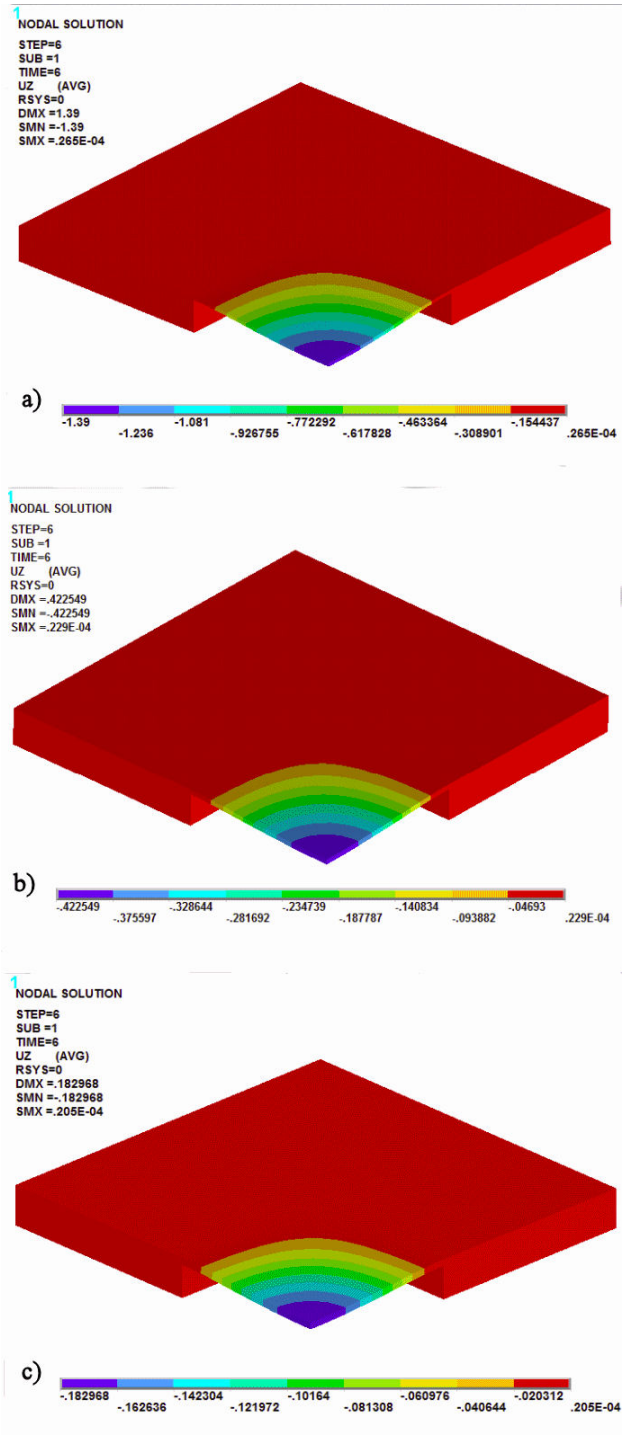

FIGURE 7. Deflection distribution (μm) of a FEM model of a piezoresistive pressure microsensor with a square-shaped diaphragm (1000 μm length) under an uniform normal pressure (15 kPa) and considering thicknesses of 10, 15, and 20 μm.

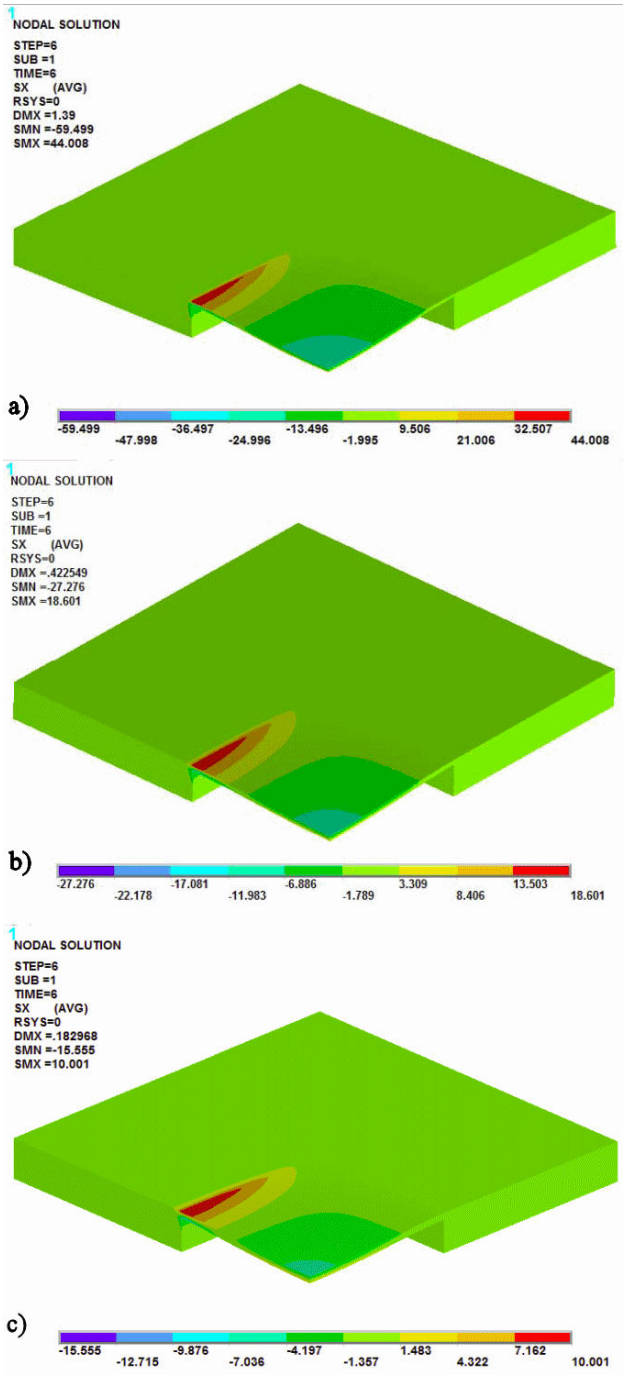

FIGURE 8. Normal stress distribution (MPa) obtained using a FEM model of a piezoresistive pressure microsensor with a square-shaped diaphragm (1000 μm length) under a uniform normal pressure (15 kPa) and considering thicknesses of 10, 15, and 20 μm.

diaphragm where the parallel piezoresistors are located. The center of the diaphragm is subjected to compressive-type stresses, of which the highest compressive stress was 20.40 MPa.

A FEM model of the same piezoresistive pressure microsensor was made through ANSYS and its mechanical behavior was compared with the polynomial model and the Timoshenko model. The FEM model represents one quarter of the pressure microsensor (due to symmetry conditions) in order to decrease the computer time. First, the model was drawn using CAD software (Solid Edge17) and after that was transferred to ANSYS software. Then, the load and mesh conditions were applied to this FEM model with elements

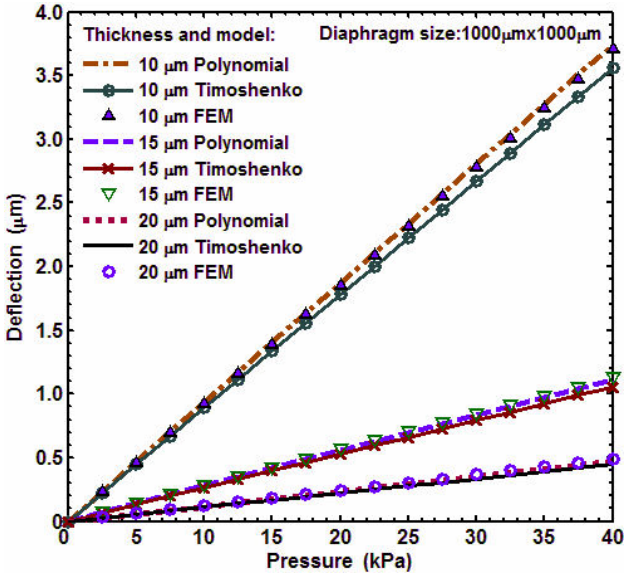

FIGURE 9. Maximum deflections variation versus pressure applied to a piezoresistive pressure microsensor with a square-shaped diaphragm (1000 μm length) and considering thicknesses of 10, 15, and 20 μm.

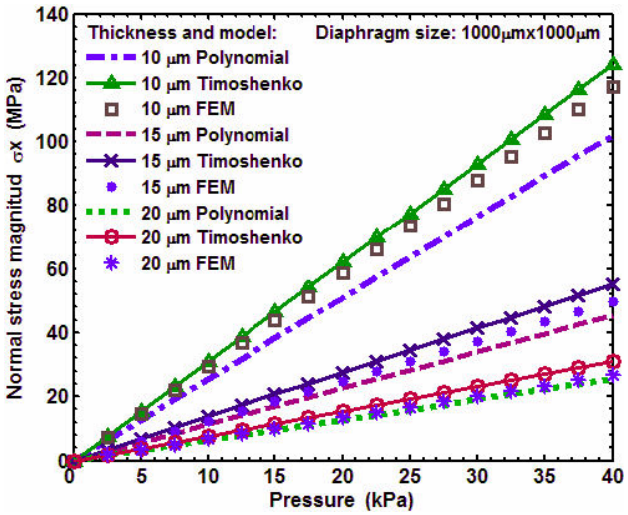

FIGURE 10. Maximum normal stress variation (σ_x) versus pressure applied to a piezoresistive pressure microsensor with a square-shaped diaphragm (1000 μm length) and considering thicknesses of 10, 15, and 20 μm.

type solid95 with three degrees of freedom each. Finally, the FEM model was solved and its electromechanical behavior was obtained for a pressure range from 0 to 40 kPa. This FEM model was made and solved in an approximate time of four hours. This computation time is greater than the time used by the polynomial model and the Timoshenko model. For the polynomial model, it took about 20 minutes to capture Eqs. (9), (20), (34), and (37) with Matlab software and to define the load and material conditions. In addition, the Matlab software needed approximately four seconds to solve these equations. However, the time taken for the Timoshenko

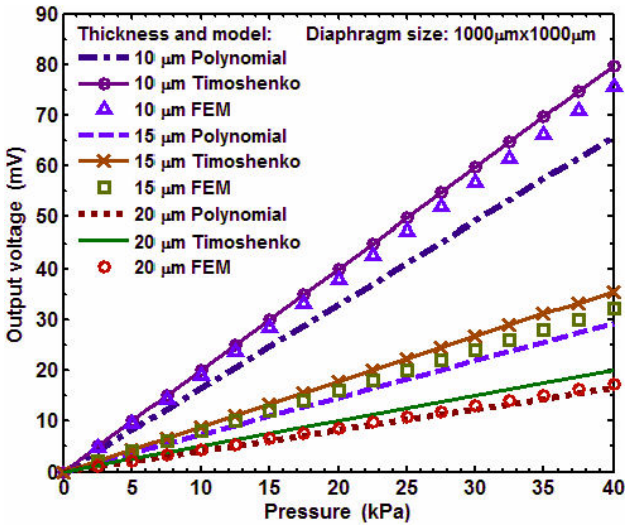

FIGURE 11. Output voltage variation of a Wheatstone bridge versus pressure applied to a piezoresistive pressure microsensor with a square-shaped diaphragm (1000 μm length) and considering thicknesses of 10, 15, and 20 μm.

model to be captured with Matlab software was about twice as long as the time needed for the polynomial model.

First, the deflection distribution of the FEM model of the microsensor was found by considering a square-shaped diaphragm (1000 μm length) in three different thicknesses (10, 15, and 20 μm). Figure 7 shows the results of the deflection distribution of this microsensor under a uniform normal pressure of 15 kPa. The maximum deflection (1.39 μm) was found in the diaphragm 10 μm thick. This value is 3.29 and 7.60 times greater than that obtained in the diaphragms with 15 and 20 μm of thickness, respectively. In addition, the normal stress distribution for the same diaphragm with three different thicknesses (10, 15, and 20 μm) was recorded, as shown in Fig. 8. The maximum tensile stress (44.01 MPa) is located at the middle edge of the diaphragm 10 μm thick. This value is 2.37 and 4.40 higher than that found in the diaphragms 15 and 20 μm thick, respectively. The stress distribution decreases and becomes compressive at the center of the diaphragm. In both cases, the stresses are less than the rupture stress of 360 MPa in $\langle 100 \rangle$ silicon [26].

Figure 9 shows the deflections of the pressure microsensor considering three different thicknesses (10, 15, and 20 μm) and a uniform normal pressure from 0 to 40 kPa. These deflections were obtained at the diaphragm center using the polynomial model, the Timoshenko model and the FEM model. The results of the polynomial model agree well with the other two models. The diaphragm 10 μm thick exhibits a maximum deflection of 3.74 μm using the polynomial model, which has a relative difference of 5.14 and 0.92% with respect to the Timoshenko model and the FEM model, respectively. The deflections for the diaphragms 15 and 20 μm thick showed a reduction of 70.38 and 87.50% with respect to the thickness of 10 μm.

TABLE I. Sensitivity of a piezoresistive pressure microsensor with a square-shaped diaphragm obtained using the polynomial model, the Timoshenko model and the FEM model.

Diaphragm parameter		Sensitivity (mV/V/kPa)		
Length (μm)	Thickness (μm)	Polynomial model	Timoshenko model	FEM model
1000	10	1.64	1.99	1.89
1000	15	0.73	0.89	0.80
1000	20	0.41	0.50	0.43

The result of the maximum normal stresses (σ_x) in the diaphragm of the microsensor is shown in Fig. 10. This response was obtained using the polynomial model, the Timoshenko model and the FEM model. For a pressure lower than 20 kPa and a thickness greater than 10 μm, the maximum normal stress calculated using the polynomial model agrees well with the other two models. For the diaphragm 15 μm thick, the polynomial model showed a maximum stress of 45.37 MPa versus 55.17 and 49.60 MPa obtained with the Timoshenko model and the FEM model, respectively. These values are less than the rupture stress of $\langle 100 \rangle$ silicon [26]. Moreover, the diaphragm 10 μm thick exhibited the highest normal stress (102.1 MPa using the polynomial model and 124.1 MPa using the Timoshenko model).

The results of the normal stress components obtained by the three models (polynomial, Timoshenko and FEM models) were introduced into Eq. (34) to find the electric behavior of the Wheatstone bridge of the pressure microsensor. Figure 11 shows the output voltage of the Wheatstone bridge versus the pressure (0-40 kPa) applied to the diaphragm. In this case, a supply voltage (V_{in}) of 1 V and three different thicknesses for the diaphragm were considered. For the two thicknesses with higher magnitude (15 and 20 μm), the results obtained with the polynomial model agree well with the Timoshenko model and the FEM model. In addition, the results of sensitivity (mV/V/kPa) of the pressure microsensor are shown in Table I. The highest sensitivity was calculated for the diaphragm 10 μm thick. Using the polynomial model, the diaphragm 10 μm thick has a maximum sensitivity of 1.64 mV/V/kPa, while the two diaphragms that are 15 μm and 20 μm thick have sensitivities of 0.73 mV/V/kPa and 0.41 mV/V/kPa, respectively. Therefore, the electromechanical design of the piezoresistive pressure microsensor showed that the square-shaped diaphragm 1000 μm length and 10 μm thickness has an adequate sensitivity and a safe mechanical response for measuring blood pressure and heart rate in the pressure range from 0 to 40 kPa. This design was obtained using the proposed polynomial model with a lower computing time than the Timoshenko model and the FEM model.

4. Conclusions

A novel polynomial model was developed to predict the electromechanical behavior of piezoresistive pressure microsensors with square-shaped diaphragms more easily and quickly for low-pressure biomedical applications. This model was determined using the small-deflection theory for the bending of thin plates and the Ritz method. The expressions of the polynomial model are simpler than the classical Timoshenko model for plates. A pressure microsensor with a square-shaped diaphragm (1000 μm length) and with three different thicknesses (10, 20, and 30 μm) was studied. For small deflections of the diaphragm, the electromechanical behavior of the pressure microsensor obtained using the polynomial model agrees well with the Timoshenko model and the FEM model. The deflections of the diaphragm (10 μm thick) calculated using the polynomial model showed a relative difference of 5.14 and 0.92% with respect to the Timoshenko model and the FEM model, respectively. In addition, the deflections of the diaphragm exhibited a reduction of 70.38 and 87.50% for thicknesses of 15 and 20 μm, respectively. A maximum sensitivity (1.64 mV/V/kPa) was calculated for the diaphragm 10 μm thick.

Acknowledgements

This work was supported by the University of Guanajuato (UG DINPO project 099/2008) and CONACYT through project 84605. We would also like to thank Prof. Jerry Hemmye of Western Michigan University for useful discussions and suggestions.

1. C. Pramanik, H. Saha, and U. Gangopadhyay, *J. Micromech. Microeng.* **16** (2006) 2060.
2. S. Marco, J. Samitier, O. Ruiz, J.R. Morante, and J.E. Steve, *Meas. Sci. Technol.* **7** (1996) 1195.
3. B.H. Bae, *et al., J. Micromech. Microeng.* **13** (2003) 613.
4. G.H. Mohamed, *MEMS Handbook* (Boca Raton, FL: CRC Press, 2002).
5. R. Schlierf, *et al., J. Micromech. Microeng.* **17** (2007) S98.
6. A.V. Chavan and K.D. Wise, *J. Microelectromech. Syst.* **10** (2001) 580.
7. Z. Yan-Hong, *et al., IEEE Sensors J.* **7** (2007) 1742.
8. J.K. Otto, T.D. Brown, and J.J. Callaghan, *Exp. Mech.* **39** (1999) 317.
9. G. Bistué, *et al., J. Micromech. Microeng.* **7** (1997) 244.
10. J. Jordana and A.R. Pallàs-Areny, *Sens. Actuators A* **127** (2006) 69.
11. Y. Kanda and A Yasukawa, *Sens. Actuators A* **62** (1997) 539.
12. T. Lisec, M. Kreutzer, and B. Wagner, *IEEE Trans. Electron Dev.* **43** (1996) 1447.

13. S. Beeby, G. Ensell, M. Kraft, and N. White, *MEMS Mechanical sensors* (Norwood, MA: Artech House, 2004).
14. H.P. Le, K. Shah, J. Singh, and A. Zayegh, *Analog Integr. Circ. Sig. Process.* **48** (2006) 21.
15. N. Maluf, *An Introduction to Microelectromechanical Systems Engineering* 2nd ed. (Norwood, MA: Artech House, 2004).
16. L. Lin and W. Yung, *Mechatronics* **8** (1998) 505.
17. L. Lin, H.C. Chu, and Y.W. Lu, *J. Microelectromech. Syst.* **8** (1999) 514.
18. G. Bistué, *et al.*, *Sens. Actuators A* **62** (1997) 591.
19. C. Gin-Shin, J. Ming-Shaung, and F. Yean-Kuen, *Sens. Actuators A* **86** (2000) 108.
20. A.C. Ugural, *Stresses in Plates and Shells* (New York: McGraw Hill, 1981).
21. E. Ventsel and T. Krauthammer, *Thin Plates and Shells: Theory, Analysis, and Applicatio*ns (New York: CRC Press, 2001).
22. R. Szilard, *Theories and Applications of Plate Analysis: Classical, Numerical and Engineering Methods* (New Jersey: John Wiley & Sons, 2004).
23. S.P. Timoshenko and S. Woinowsky-Krieger, *Theory of Plates and Shells* (New York: McGraw-Hill, 1959).
24. S.K. Clark and K.D. Wise, *IEEE Trans. Electron Dev.* **26** (1979) 1887.
25. T. Toriyama and S. Sugiyama, *J. Microelectromech. Syst.* **11** (2002) 598.
26. J.M. Borky, *Silicon Diaphragm Pressure Sensors with Integrated Electronics*, (Ph. D. Thesis, University of Michigan, Ann Arbor, 1997).